Vibrational Overtone Stretching Transitions in Sarin

Michael W. P. Petryk

Defence Research & Development Canada – Suffield, Alberta, Canada

ABSTRACT

The CH stretching overtone transitions of the nerve agent sarin (O-isopropyl methylphosphonofluoridate) are of interest to the standoff detection of chemical warfare agents, as many of these transitions occur near regions where small, efficient, portable diode lasers (originally developed for use in the telecommunications industry) operate. However, the interpretation of experimental vibrational overtone spectra is often difficult, and the computational simulation of overtone transitions in a molecule is challenging. Presented herein are the simulated CH overtone stretching transitions in sarin. Spectral regions are simulated from overtone transition energies and intensities, both of which are calculated within the harmonically coupled anharmonic oscillator (HCAO) model. Data for HCAO calculations are obtained from *ab initio* calculations, without any recourse to experimental data.

Keywords: local mode, vibrational overtone, anharmonic oscillator, sarin, nerve agent, isopropyl methylphosphonofluoridate

1. INTRODUCTION

In sarin there are ten nonequivalent CH oscillators; this situation significantly complicates the assignment of experimentally observed CH stretching overtone transitions, necessitating recourse to a theoretical prediction of the spectrum of the overtone transitions. Fortunately, the XH (where X is any atom heavier than H) stretching vibrational overtone transitions in molecules are well-approximated by the harmonically coupled anharmonic oscillator (HCAO) model.[1,2] Within this model the XH oscillators of a molecule are treated as a collection of isolated anharmonic oscillators, and the couplings between these oscillators are treated as perturbations. The HCAO model has been used to accurately predict and interpret the stretching vibrational overtone spectra of molecules whose local mode parameters are known.[3–5] *Ab initio* calculations allow the prediction of overtone spectra for molecules which have not been observed experimentally.[6,7] An excellent review of the HCAO model and local modes of vibration has been published by Henry and Kjaergaard.[8]

2. THEORY AND CALCULATIONS

2.1. Local Modes of Vibration and the HCAO Model

Vibrational overtone spectra of CH stretches can be interpreted within the local mode model of molecular vibration.[9,10] Within this model the CH stretching potential, $V(q)$, is frequently approximated by a Morse potential[11]

$$V(q) = D_e(1 - \mathrm{e}^{-aq})^2 \tag{1}$$

where q is displacement from the equilibrium CH bond length, D_e is the depth of the potential energy well, and a is the Morse scaling factor. The potential energy well depth is given by

$$D_e = \frac{\tilde{\omega}^2}{4\tilde{\omega}x}. \tag{2}$$

The terms $\tilde{\omega}$ and $\tilde{\omega}x$ are the pure local mode frequency and anharmonicity (*vide infra*), respectively, while the Morse scaling factor a is given by

$$a = \frac{\tilde{\omega}}{\hbar}\sqrt{\frac{\mu}{2D_e}} \tag{3}$$

Further author information: (Send correspondence to M.W.P.P.)
M.W.P.P.: E-mail: Michael.Petryk@drdc-rddc.gc.ca, Telephone: 1 403 544 4494, Facsimile: 1 403 544 3388

Chemical and Biological Sensors for Industrial and Environmental Monitoring II
edited by Steven D. Christesen, Arthur J. Sedlacek III, James B. Gillespie, Kenneth J. Ewing
Proc. of SPIE Vol. 6378, 637818, (2006) · 1605-7422/06/$15 · doi: 10.1117/12.685015

where μ is the reduced mass of the CH oscillator. The energy eigenvalues of a Morse oscillator, $\widetilde{E}_\upsilon$, are[11,12]

$$\widetilde{E}_\upsilon = \widetilde{\omega}\left(\upsilon + \frac{1}{2}\right) - \widetilde{\omega}x\left(\upsilon + \frac{1}{2}\right)^2. \tag{4}$$

This equation can be rearranged to give the frequency, $\widetilde{\nu}_{\upsilon\leftarrow 0}$, of an overtone transition out of the ground state, $(\upsilon' = \upsilon) \leftarrow (\upsilon'' = 0)$[11]

$$\widetilde{\nu}_{\upsilon\leftarrow 0} = \upsilon\widetilde{\omega} - (\upsilon^2 + \upsilon)\widetilde{\omega}x. \tag{5}$$

Transitions out of the ground vibrational state into a state excited by n vibrational quanta are often reported in terms of the change in the number of vibrational quanta and expressed as $\Delta\upsilon_{\mathrm{CH}} = n$.

The experimental values of the Morse parameters $\widetilde{\omega}$ and $\widetilde{\omega}x$ are obtained either from a Birge–Sponer plot of $\widetilde{\nu}_{\upsilon\leftarrow 0}/\upsilon$ *vs.* υ or from a quadratic fit of $\widetilde{\nu}_{\upsilon\leftarrow 0}$ *vs.* υ. In the absence of experimental data, $\widetilde{\omega}$ and $\widetilde{\omega}x$ can be calculated from *ab initio* data (*vide infra*). The vibrational eigenstates are obtained within the HCAO model[1,2,13,14] in terms of Morse oscillator wavefunctions[11] with the assumption of harmonic coupling between the CH oscillators.

2.2. Coupled CH Oscillators

The (unsymmetrized) wavefunction of k coupled local mode CH oscillators excited by υ vibrational quanta can be expressed as $|\upsilon_1, \upsilon_2, \ldots, \upsilon_k\rangle$ where $\upsilon = \upsilon_1 + \upsilon_2 + \ldots + \upsilon_k$. The sum total of the number of vibrational quanta of excitation is often referred to as the vibrational manifold. Since electromagnetic fields select transitions into states where all the vibrational quanta are localized in one of a set of equivalent CH oscillators (*i. e.*, into states $|\upsilon, 0, \ldots, 0\rangle$, $|0, \upsilon, \ldots, 0\rangle$, *etc.*), we can denote the unsymmetrized wavefunction of k identical coupled local mode CH oscillators as simply $|\upsilon\rangle$. The frequency of transitions out of the ground $|0\rangle$ state to the state $|\upsilon\rangle$ for an isolated CH oscillator is given by Equation (5). For a molecule with coupled oscillators the equivalent energy expression, given in terms of the molecular Hamiltonian, H, is[1]

$$\frac{H - E_{|0\rangle}}{hc} = \sum_i^k \upsilon_i\widetilde{\omega}_i - \sum_i^k \left(\upsilon_i^2 + \upsilon_i\right)\widetilde{\omega}x_i - \sum_{i\neq j}^k \gamma'_{ij}\left(a_i a_j^+ + a_i^+ a_j\right) \tag{6}$$

where a^+ and a are (respectively) the creation and annihilation operators, $E_{|0\rangle}$ is the energy of the vibrational ground state and γ'_{ij} is the intramanifold coupling parameter[1]

$$\gamma'_{ij} = (\gamma_{ij} - \phi_{ij})\sqrt{\widetilde{\omega}_i\widetilde{\omega}_j} \tag{7}$$

where γ_{ij} and ϕ_{ij} are, respectively, the kinetic and potential energy coupling terms of coupled oscillators CH_i and CH_j. These terms can be expressed as[1]

$$\phi_{ij} = \frac{1}{2}\frac{F_{ij}}{F_{ii}F_{jj}} \tag{8}$$

and

$$\gamma_{ij} = -\frac{1}{2}\frac{G_{ij}}{G_{ii}G_{jj}} \tag{9}$$

where F and G terms represent the well-known Wilson matrix elements.[15] The non-diagonal force constant F_{ij} can be obtained from an *ab initio* potential energy surface (PES) along a two stretch coordinates while the diagonal force constants F_{ii} and F_{jj} can each be derived from *ab initio* PESs along a single stretch coordinate.[16] The term γ_{ij} is a function of molecular conformation only, and can be expressed as[1]

$$\gamma_{ij} = -\frac{1}{2}\cos(\theta)\left(1 + \frac{m_{\mathrm{C}}}{m_{\mathrm{H}}}\right)^{-1} \tag{10}$$

where θ is the H–C–H bond angle of the coupled oscillators and m_{C} and m_{H} are the atomic masses of C and H. The values of $\widetilde{\omega}$ and $\widetilde{\omega}$ used in Equations (6) and (7) can be obtained from Equation (5) (or variants thereof), or they can be obtained from *ab initio* calculated PESs.[17,18] Finally, the value of θ in Equation (10) can be calculated *ab initio*.

2.3. Oscillator Strength

Within the double harmonic approximation (*i. e.*, harmonic restoring potential and linear dipole moment function) overtone transitions are forbidden. However, the restoring potential of a real molecule is somewhat anharmonic and the dipole moment function (DMF) of a real molecule is somewhat nonlinear, allowing vibrational overtone transitions to occur. The experimental intensities of vibrational overtone transitions can be expressed in terms of the dimensionless oscillator strength, f_{osc}.[19] By applying the ideal gas law and using appropriate physical constants[20] f_{osc} can be expressed in the form

$$f_{\text{osc}} = 2.6935 \times 10^{-9}(\text{Torr m cm})\frac{T}{p\,l}\int A(\tilde{\nu}_{eg})\mathrm{d}(\tilde{\nu}_{eg}) \tag{11}$$

where T is the temperature of the gas (in Kelvin), p is the gas pressure (in Torr), l is the path length (in meters), and $A(\tilde{\nu}_{eg})$ is the absorbance of the transition from ground state g to excited state e as a function of frequency, $\tilde{\nu}_{eg}$, expressed in wavenumbers (cm^{-1}). The integration is carried out over the range of the absorption feature. Similarly, the oscillator strength of an overtone transition can be calculated from the expression[19]

$$f_{\text{osc}} = 4.70175 \times 10^{-7}(\text{cm D}^{-2})\tilde{\nu}_{eg}|\boldsymbol{\mu}_{eg}|^2 \tag{12}$$

where the term 4.70175×10^{-7} denotes a collection of appropriate physical constants,[20] $\tilde{\nu}_{eg}$ represents the transition frequency, and $\boldsymbol{\mu}_{eg}$ is the transition dipole moment matrix element (*vide infra*), expressed in Debye (D).

2.4. The Dipole Moment Function

The transition dipole moment matrix element (in Debye) is given by

$$\boldsymbol{\mu}_{eg} = \langle e|\vec{\mu}|g\rangle \tag{13}$$

where e and g are the excited and ground state wavefunctions, respectively, and $\vec{\mu}$ denotes the DMF (*vide infra*). As noted previously, the wavefunction of a Morse oscillator excited by υ vibrational quanta can be calculated from the reduced mass μ, and the local mode parameters $\tilde{\omega}$ and $\tilde{\omega}x$.[11]

Within the HCAO model, couplings between adjacent CH oscillators (*vide supra*) are treated as pairwise interactions between the internal displacement coordinates q_1 along CH_1 and q_2 along CH_2. *Ab initio* calculations have been used[21–25] to obtain discrete dipole moment values as functions of q_1 and q_2. In this paper the dipole moment values were calculated as q_1 and q_2 were stretched or compressed about their equilibrium CH bond lengths, r_e, by $\pm$ 0.30 Å in increments of 0.05 Å with all other molecular coordinates held constant at their equilibrium values. The continuous DMF of two coupled CH oscillators along their internal stretch coordinates q_1 and q_2 is approximated by a Taylor series expansion taken up to sixth order

$$\vec{\mu}(q_1, q_2) = \sum_{i,j=1}^{i+j=6} \vec{\mu}_{ij} q_1^i q_2^j \tag{14}$$

where $\vec{\mu}_{ij}$ are the DMF derivatives

$$\vec{\mu}_{ij} = \frac{1}{i!j!}\frac{\partial^{i+j}\vec{\mu}}{\partial q_1^i \partial q_2^j} \tag{15}$$

which were obtained from a polynomial fit to *ab initio* values of the dipole moment. Terms in Equation (14) include the pairwise mixed derivatives $\partial^2\vec{\mu}/\partial q_1^1 \partial q_2^1$, $\partial^3\vec{\mu}/\partial q_1^1 \partial q_2^2$, and $\partial^3\vec{\mu}/\partial q_1^2 \partial q_2^1$. It is especially important to include terms beyond those which are linear in q as the second order derivatives $\partial^2\vec{\mu}/\partial q_1^2$ and $\partial^2\vec{\mu}/\partial q_2^2$ can contribute significantly more intensity to overtone transitions than the linear terms.

It is known that DMFs obtained from *ab initio* calculations are of higher quality if computer resources are spent on larger basis sets rather than on increased levels of electron correlation.[26] For vibrational overtone transitions above the second vibrational overtone, electron correlation effects on the DMF are negligible.[3,26,27] In general, it is found that Hartree-Fock (HF) theory gives excellent DMFs for the purpose of HCAO calculations of CH stretching vibrational overtone intensities.

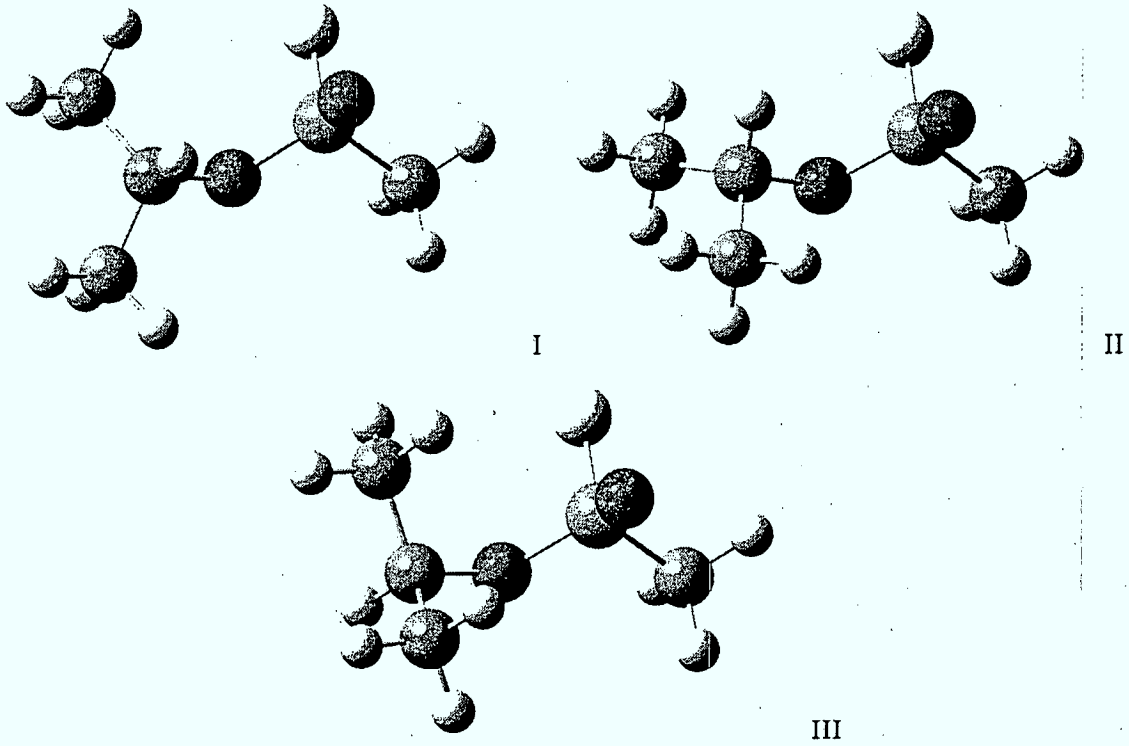

Figure 1. The structures of the three lowest energy conformers of sarin, calculated at HF / 6-311++G(2d,2p). The *S* enantiomer of sarin is shown. The top left structure, denoted I, corresponds to the lowest energy conformer of sarin while the top right structure, denoted II, corresponds to the next highest energy conformer. The bottom structure, denoted III, corresponds to the next highest energy conformer which lies above conformer II.

2.5. Computational Details

Ab initio calculations were carried our with Gaussian 03, Revision C.02[28] on an HP AlphaServer ES40 cluster with 670 MHz and 830 MHz 64-bit processors. Calculations used all Gaussian defaults except that the Gaussian overlay option IOP(3/32=2) was used with all calculations to prevent the reduction of the expansion set. All calculations were carried out using SCF=Tight because the 6-311++G(2d,2p) basis set used in this paper contains diffuse functions.

For each conformer of interest the CH stretch coordinate, q, was treated in the displacement range $q \in [-0.30, 0.30]$ Å in steps of 0.05 Å. In each conformer of sarin there is one unpaired CH stretch coordinate and nine (asymmetric) pairwise CH stretches to consider. Thus, for each conformer $13 \times 13 \times 9 + 13 = 1534$ *ab initio* calculations were carried out. At the HF / 6-311++G(2d,2p) level this required 43 days of CPU time per processor with the hardware described above. This computation time can be reduced to under one day by using several faster processors in parallel.

3. RESULTS AND DISCUSSION

In agreement with the previous work of Kaczmarek *et al.*,[29] it was confirmed that the three lowest energy conformers of sarin have the structures depicted in Figure 1. In this paper the lowest energy sarin conformer is denoted sarin I, the second lowest energy conformer is denoted sarin II, and the third conformer is denoted sarin III.

In Figure 1, the methyl group attached to the phosphorous atom contains three CH oscillators which are denoted CH_1, CH_2, and CH_3. This methyl group is referred to as $CH_{3,\alpha}$. That oscillator which lies approximately in the plane of the page is CH_1. The oscillator which points into the plane of the page is CH_2 while that which

points out of the plane is oscillator CH_3. The isopropyl methyl group which is approximately oriented towards the top left-hand side of the page comprises CH_4, CH_5, and CH_6. This methyl group is referred to as $CH_{3,\beta}$. Of these oscillators, CH_4 is that which is oriented towards the top right-hand side of the page. The oscillator CH_5 is oriented out of the plane of the page while CH_6 is oriented into the plane of the page. The remaining isopropyl methyl group, $CH_{3,\gamma}$, comprises CH_7, CH_8, and CH_9. Oscillator CH_7 is that which is oriented into the plane of the page and downwards. The orientation of CH_8 is towards the left-hand side of the page and out of its plane while CH_9 is oriented towards the right-hand side of the page and out of the plane. The isolated CH oscillator which contains the secondary carbon of the isopropyl group is denoted CH_{10}. There are two oxygen atoms in sarin: O_1 denotes that atom which is bound to both carbon and phosphorous while O_2 denotes that which is bound to phosphorous only. The geometric parameter which most clearly distinguishes the conformers of sarin is the dihedral angle (through the molecular skeleton) between the H atom in CH_{10}, denoted H_{10}, and the phosphorous atom. This characteristic angle, $\angle H_{10}$–C–O_1–P, is presented for the three sarin conformers in Table 1.

Table 1. Selected *ab initio* geometric parameters and relative energies of the lower energy conformers of sarin calculated at HF / 6-311++G(2d,2p)

	Conformer		
Parameter	I	II	III
Geometries			
$\angle H_{10}$–C–O_1–P[a]	-28°	18°	168°
$dH_{me}\cdots O_2$[b]	2.91 Å	3.01 Å	2.66 Å (2.80 Å)
$dH_7\cdots O_2$	3.02 Å	3.02 Å	3.01 Å
$dH_9\cdots O_2$	3.03 Å	3.04 Å	3.03 Å
$dH_{10}\cdots O_2$	2.56 Å	2.74 Å	N/A[c]
$dH_7\cdots F$	2.91 Å	3.50 Å	3.11 Å
$dH_9\cdots F$	3.69 Å	4.49 Å	2.97 Å
$dH_{10}\cdots F$	3.61 Å	3.07 Å	4.02 Å
Relative Energies[d]			
ΔE	0 cm^{-1}	46.6 cm^{-1}	675 cm^{-1}
ΔE_{ZPVE}	0 cm^{-1}	29.7 cm^{-1}	719 cm^{-1}

[a] These parameters pertain to the *S* enantiomer of sarin.
[b] H_{me} denotes the methyl hydrogen atom closest to atom O_2. In sarin I, H_{me} is H_4, in sarin II H_{me} corresponds to H_6, while for sarin III H_{me} corresponds to either of two nearly equidistant atoms, H_6 and H_7 (the former value appears in parentheses).
[c] Through-space interactions between H_{10} and O_2 are not possible as the atoms are on opposite sides of the molecule.
[d] Energies ΔE have not been ZPVE corrected while ΔE_{ZPVE} values have been ZPVE corrected.

Ab initio calculated geometries and van der Waals radii can be used as crude metrics to quantify the relative degree of steric crowding in a molecule.[18] The nonbonded, internuclear separations between a hydrogen atom H_i and an electronegative atom Y (where Y=F or O), denoted $dH_i\cdots Y$, are presented in Table 1 for several atom pairs. The van der Waals radii of hydrogen, fluorine, and oxygen are, respectively, 120 pm, 135 pm, and 140 pm.[30] It is known that CH stretching potentials become more harmonic with increases in steric crowding[31–34] as a result of intramolecular coupling through space between proximal, nonbonded atoms.[34,35] Thus, internuclear separations $dH_i\cdots Y$ of approximately 2.6 Å or less are sufficiently small that nonbonded interactions through

space are likely to perturb the molecule's vibrational overtone spectrum. Such through-space interactions are likely to occur over larger internuclear separations where the large amplitude stretching motions which accompany transitions to high vibrational overtones are accompanied by methyl libration.[34] One consequence of through-space coupling in initially prepared vibrational stretching overtone states is the rapid de-excitation of that excited state *via* intramolecular vibrational energy redistribution (IVR).[11,36] A spectral manifestation of IVR is peak broadening owing to lifetime uncertainty, resulting in a Lorentzian profile. Based upon the similarity of the internuclear separations $d\mathrm{H}_i \cdots Y$ presented in Table 1 with those in the *tert*-butyl halides,[18] reasonable estimates of the full-width at half-maximum (FWHM) values of the Lorentzian profiles of the vibrational overtone transitions in sarin are 40 cm^{-1} at $\Delta\upsilon_{\mathrm{CH}} = 3$, 60 cm^{-1} at $\Delta\upsilon_{\mathrm{CH}} = 4$, and 70 cm^{-1} at $\Delta\upsilon_{\mathrm{CH}} = 5, 6$. The HCAO calculated vibrational overtone spectral profiles of sarin have been simulated using FWHM values slightly lower than the aforementioned widths so as not to obscure detail unnecessarily.

The relative energies of conformers I–III of sarin, calculated at HF / 6-311++G(2d,2p), are presented in Table 1. The term ΔE_{ZPVE} represents the zero point vibrational energy (ZPVE) corrected energy (at 298.15 K and 1.00 atm pressure) relative to sarin I while ΔE represents the non-ZPVE corrected relative energy. The ZPVE corrected relative energy of sarin II was determined to be 29.7 cm^{-1}, which is in good agreement with that reported by Kaczmarek *et al.*,[29] who found the energy difference to be 31.48 cm^{-1} at MP2 / 6-311++G(d,p). The agreement between the ΔE_{ZPVE} value of sarin III in Table 1, which was determined to be 719 cm^{-1}, and that reported by Kaczmarek *et al.*[29] as 454.68 cm^{-1}, is unexpectedly poor. However, Hight Walker *et al.*[37] reported a ΔE_{ZPVE} value for sarin III to be 604.5 cm^{-1} at HF / 6-311G(d,p) and 500.8 cm^{-1} at MP2 / 6-311G(d,p). The inclusion of some electron correlation through the use MP2 theory is seen to have a pronounced effect on the relative energy of the sarin III conformer. The relative energies of the conformers of sarin in Table 1 have been used to determine their relative populations at 298 K for the purpose of scaling their relative contributions to the room temperature overtone spectrum of sarin.

As noted in the Introduction, the HCAO model can accurately predict: (1) relative absorbance intensities among oscillators within a molecule; and (2) absolute absorbance intensities, which accompany vibrational overtone transitions. However, the presence of low barriers to internal methyl rotation can greatly complicate the overtone spectrum of a molecule by allowing the possibility of hundreds of transitions which may contribute to the observed spectral profile.[38–40] In conformer I the barriers to internal methyl torsion were 730 cm^{-1} for $\mathrm{CH}_{3,\alpha}$, 1310 cm^{-1} for $\mathrm{CH}_{3,\beta}$, and 1330 cm^{-1} for $\mathrm{CH}_{3,\gamma}$ while those barriers in conformer II were 690 cm^{-1}, 1340 cm^{-1}, and 1370 cm^{-1}, respectively. Visualization of the *ab initio* output indicates that no major skeletal motions have accompanied methyl torsion. These barriers are only approximate: they have not been ZPVE corrected and no scaling factors have been applied. Nevertheless, they are sufficiently high that free methyl rotation will not complicate the observed overtone spectra.

In order to calculate the overtone transition oscillator strength with Equation (12), the transition dipole moment was calculated from Equation (13) using the Morse wavefunctions as defined by the vibrational quantum number, υ, the local mode frequency, $\widetilde{\omega}$, and the local mode anharmonicity, $\widetilde{\omega}x$.[11] The local mode parameters $\widetilde{\omega}$ and $\widetilde{\omega}x$ for the two lowest energy conformers of sarin were determined from a nonlinear fit of an *ab initio* PES to Equation (1). All *ab initio* PESs were calculated at HF / 6-311++G(2d,2p) in the CH displacement range $q \in [-0.20, 0.20]$ Å in steps of 0.05 Å and scaled by $sf_{\widetilde{\omega}} = 0.9429 \pm 0.0015$ for $\widetilde{\omega}$ and $sf_{\widetilde{\omega}x} = 0.921 \pm 0.015$ for $\widetilde{\omega}x$.[18] The local mode parameters for sarin I and II are presented in Table 2. Note that the highest local mode anharmonicity occurs in CH_{10}, which is expected on the bases of the small internuclear separations between H_{10} and the atoms O_2 and F (see Table 1). In sarin I H_{10} is in close proximity to O_2 while H_{10} is in close proximity to both O_2 and F in sarin II. There is an attractive electrostatic interaction of H_{10} with F and/or O_2. It is known that CH oscillators are perturbed by halogen substitution: CH stretching force constants have been observed to increase with halogen substitution[41] and $\widetilde{\omega}$ values are known to increase with increasing electronegativity.[42] Attractive electrostatic interactions have been observed[18,43] to lead to increased $\widetilde{\omega}x$ values and to a blue-shifting of the vibrational overtone transition frequencies. These effects are more prominent in sarin II than in sarin I as in sarin II the H_{10} atom interacts with both O_2 and F.

Table 2. *Ab initio* calculated, scaled local mode parameters[a] $\tilde{\omega}$ and $\tilde{\omega}x$ (in cm^{-1}) of the two lowest energy conformers of sarin obtained at HF / 6-311++G(2d,2p)

	Conformer			
	I		II	
Oscillator	$\tilde{\omega}$	$\tilde{\omega}x$	$\tilde{\omega}$	$\tilde{\omega}x$
CH_1	3095 ± 5	58.5 ± 1.0	3098 ± 5	58.3 ± 1.0
CH_2	3102 ± 5	58.4 ± 1.0	3103 ± 5	58.4 ± 1.0
CH_3	3101 ± 5	58.5 ± 1.0	3102 ± 5	58.3 ± 1.0
CH_4	3079 ± 5	59.1 ± 1.0	3077 ± 5	59.4 ± 1.0
CH_5	3066 ± 5	59.3 ± 1.0	3067 ± 5	59.2 ± 1.0
CH_6	3066 ± 5	59.5 ± 1.0	3066 ± 5	59.5 ± 1.0
CH_7	3065 ± 5	59.5 ± 1.0	3061 ± 5	59.5 ± 1.0
CH_8	3068 ± 5	59.2 ± 1.0	3064 ± 5	59.3 ± 1.0
CH_9	3076 ± 5	59.5 ± 1.0	3089 ± 5	58.9 ± 1.0
CH_{10}	3094 ± 5	60.0 ± 1.0	3075 ± 5	60.7 ± 1.0

[a] Local mode parameters were calculated from a nonlinear fit of *ab initio* data to Equation (1) and scaled using the appropriate scaling factors from Reference 18.

Local mode coupling parameters in Equation (7) were calculated in a manner identical to that of Kjaergaard *et al.*.[16] The parameter ϕ_{ij} was obtained from an expansion series fit of the CH stretching potential[16,17] calculated *ab initio* in the CH displacement range $q \in [-0.30, 0.30]$ Å in steps of 0.05 Å. The parameter γ_{ij} was calculated using Equation (10) and the *ab initio* molecular geometry.

Vibrational overtone spectra are often complicated by Fermi resonance interactions.[18,34,43] It is possible to predict ideal Fermi resonance frequency matching conditions,[34] however, the evaluation of the relevant coupling matrix elements is difficult and beyond the scope of this paper. Fermi resonance interactions are not included in the vibrational overtone transition energies and intensities for the $\Delta\upsilon_{CH} = 3 - 6$ transitions which are presented for the sarin I and II conformers in Tables 3 and 4 of Appendix A. As expected (*vide supra*) on the basis of the proximity of H_{10} to F and/or O_2, CH_{10} is blue-shifted in both conformers of sarin, with the larger blue-shift occurring in sarin II.

There are no equivalent CH oscillators in sarin. Thus, the wavefunction of coupled, excited CH oscillators on a methyl group can be expressed as $|\upsilon_i\rangle|\upsilon_j\rangle|\upsilon_k\rangle$ where υ_i is the number of vibrational quanta in CH_i, *etc.*. As indicated in Section 2.2, electromagnetic fields select transitions into states where all the vibrational quanta are localized in one of a set of equivalent CH oscillators. Thus, the dominant overtone transitions will be out of the ground state $|0\rangle|0\rangle|0\rangle$ into a state $|\upsilon_i\rangle|0\rangle|0\rangle$, $|0\rangle|\upsilon_j\rangle|0\rangle$, or $|0\rangle|0\rangle|\upsilon_k\rangle$. These excited states are referred to as pure local mode states as all of their vibrational energy is localized in an oscillator. Local mode/local mode combination states of the form $|\upsilon_i - 1\rangle|1\rangle|0\rangle$, $|\upsilon_i - 1\rangle|0\rangle|1\rangle$, *etc.*, can couple into the pure local mode states and steal intensity. In Tables 3 and 4 we note that the dominant transitions at each overtone in the range $\Delta\upsilon_{CH} = 3 - 6$ are transitions to pure local mode states. However, combination bands make significant contributions to the observed vibrational spectra.

The vibrational overtone spectrum of sarin was simulated from the transition intensities and frequencies in Tables 3 and 4. The intensities of the sarin I and II transitions were scaled by their relative Boltzmann populations at 298 K. Each transition was was given a Lorentzian profile with a width appropriate to the degree of vibrational excitation: 30 cm^{-1} at $\Delta\upsilon_{CH} = 3$, 40 cm^{-1} at $\Delta\upsilon_{CH} = 4$, and 50 cm^{-1} at $\Delta\upsilon_{CH} = 5, 6$. The individual Lorentzian transitions were summed to yield a simulated spectrum. The $\Delta\upsilon_{CH} = 3 - 6$ spectral profiles are presented in, respectively, Figures 2 through 5.

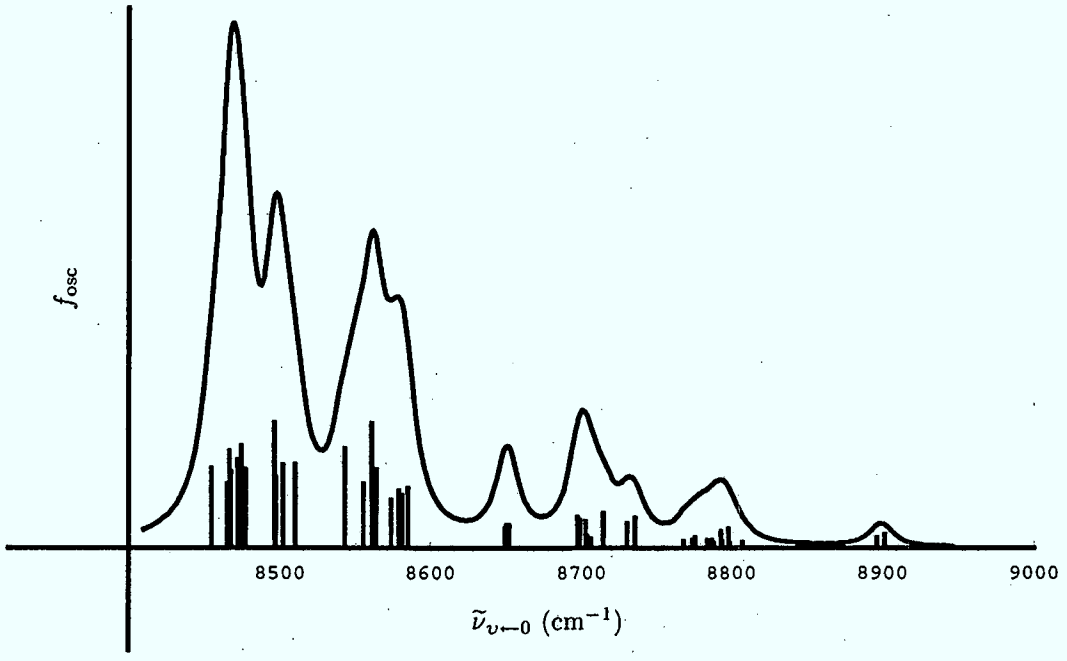

Figure 2. The $\Delta v_{CH} = 3$ HCAO calculated vibrational overtone spectral region of an equilibrium distribution of sarin I and II conformers at 298 K. The maximum (summed) absorbance feature in this region has an oscillator strength of 2.47×10^{-9} at *ca.* 8470 cm^{-1}.

The summed $\Delta v_{CH} = 3$ transition in Figure 2 has a maximum oscillator strength, f_{osc}, of 2.47×10^{-9} which occurs at *ca.* 8470 cm^{-1}. The f_{osc} values of the individual Boltzmann weighted transitions within the $v = 3$ manifold are shown in Figure 2 as vertical lines. The accurate calculation of the vibrational overtone spectrum of sarin at $\Delta v_{CH} = 3$ is seen to depend upon the contributions of pure local mode transitions as well as upon numerous local mode/local mode combination bands.

The maximum summed $\Delta v_{CH} = 4$ transition f_{osc} is 2.56×10^{-10} and is seen in Figure 3 to occur at *ca.* 11060 cm^{-1}. Numerous individual Boltzmann weighted transitions within the $v = 4$ manifold are seen to contribute to the overall profile, reinforcing the necessity to accurately treat the contributions of pure local mode states and local mode/local mode combination states.

In Figure 4 the maximum summed $\Delta v_{CH} = 5$ f_{osc} value is 2.62×10^{-11}, which occurs at *ca.* 13540 cm^{-1}, while in Figure 5 the maximum summed $\Delta v_{CH} = 6$ f_{osc} value is 3.42×10^{-12} and occurs at *ca.* 15890 cm^{-1}. In both of these frequency ranges the sum profile depends strongly upon the individual contributions of both pure local mode states and local mode/local mode combination states.

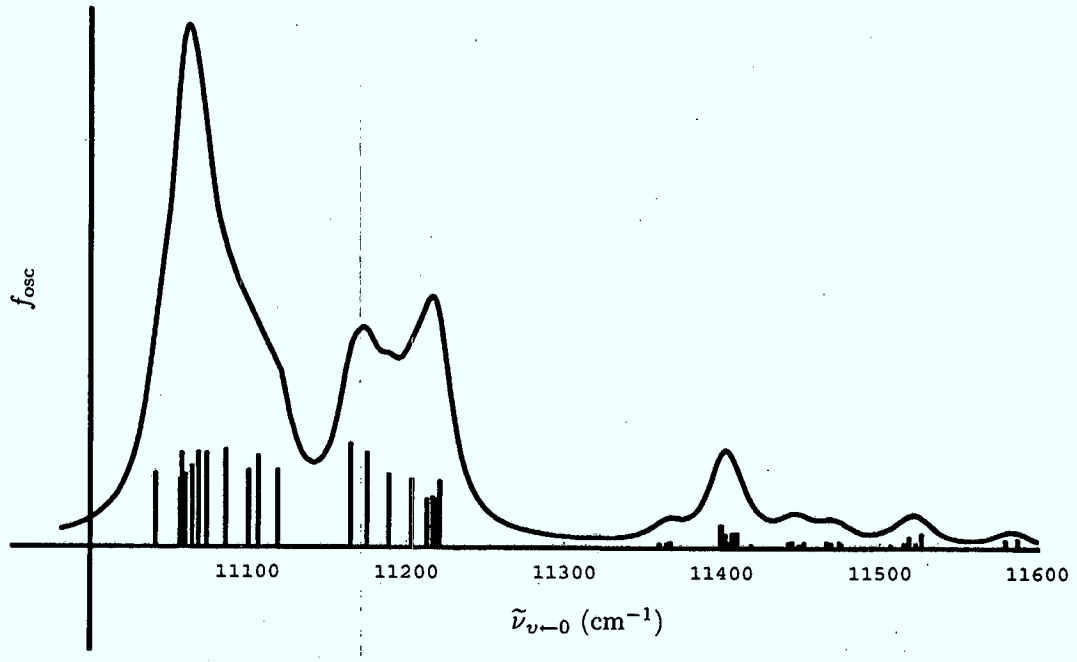

Figure 3. The $\Delta v_{CH} = 4$ HCAO calculated vibrational overtone spectral region of an equilibrium distribution of sarin I and II conformers at 298 K. The maximum (summed) absorbance feature in this region has an oscillator strength of 2.56×10^{-10} at *ca.* 11060 cm^{-1}.

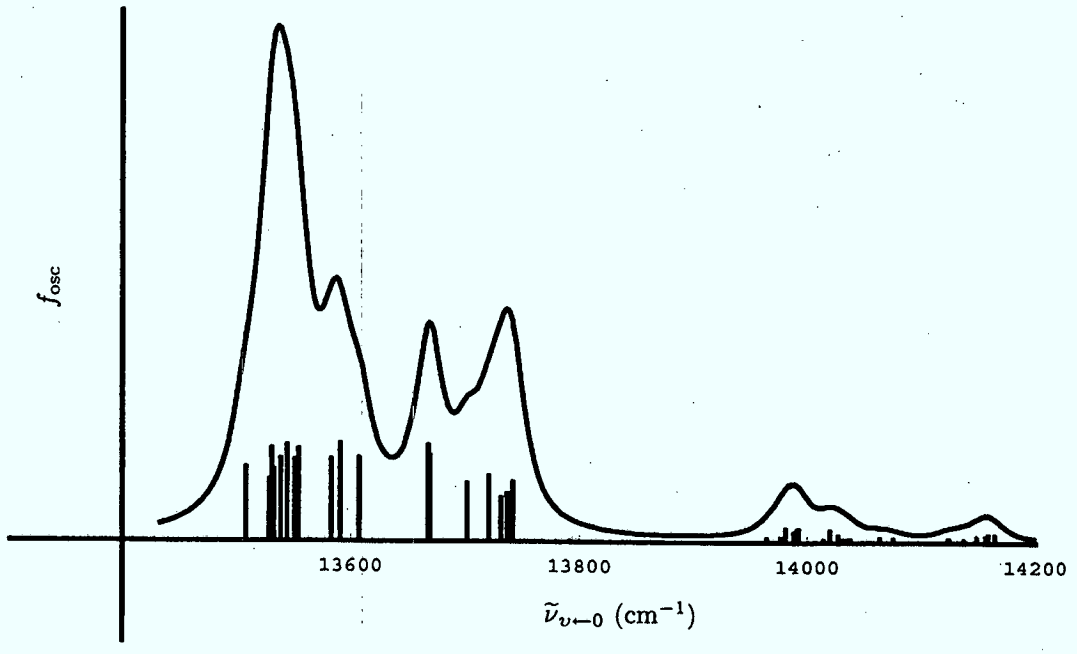

Figure 4. The $\Delta v_{CH} = 5$ HCAO calculated vibrational overtone spectral region of an equilibrium distribution of sarin I and II conformers at 298 K. The maximum (summed) absorbance feature in this region has an oscillator strength of 2.62×10^{-11} at *ca.* 13540 cm^{-1}.

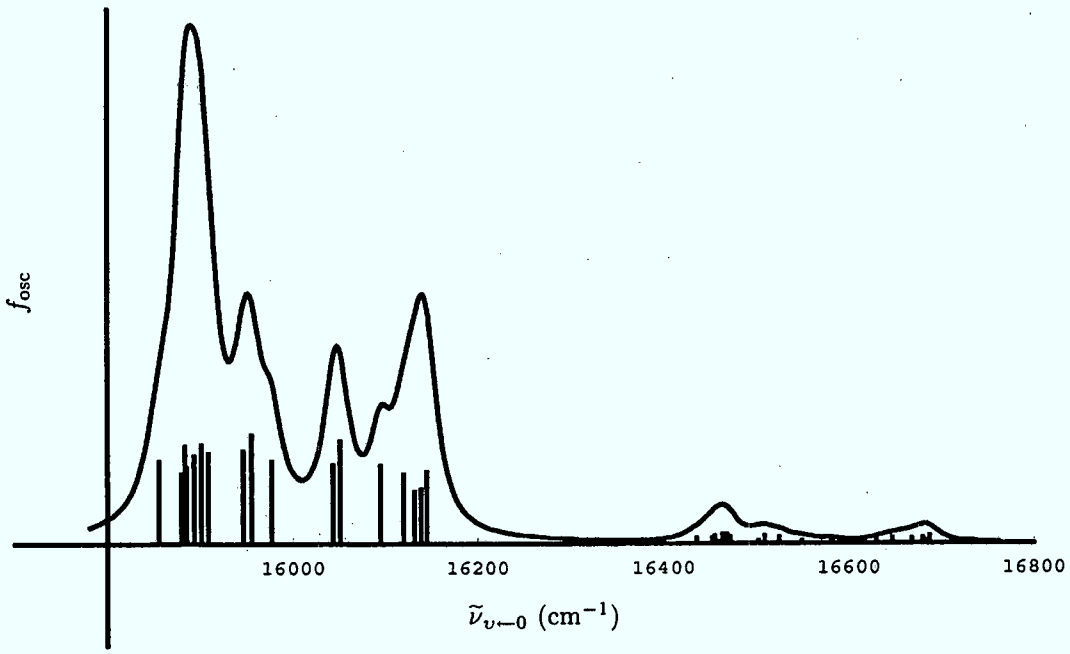

Figure 5. The $\Delta v_{CH} = 6$ HCAO calculated vibrational overtone spectral region of an equilibrium distribution of sarin I and II conformers at 298 K. The maximum (summed) absorbance feature in this region has an oscillator strength of 3.42×10^{-12} at *ca.* 15890 cm^{-1}.

APPENDIX A. CALCULATED OSCILLATOR STRENGTHS

Table 3. Transition frequencies (in cm^{-1}), $\widetilde{\nu}_{v\leftarrow 0}$, and oscillator strengths, f_{osc}, of the HCAO calculated[a] CH vibrational overtone transitions $\Delta v = 3 - 6$ in conformer I of sarin

	$\|CH_1\rangle\|CH_2\rangle\|CH_3\rangle$		$\|CH_4\rangle\|CH_5\rangle\|CH_6\rangle$		$\|CH_7\rangle\|CH_8\rangle\|CH_9\rangle$		$\|CH_{10}\rangle$	
State	$\widetilde{\nu}_{v\leftarrow 0}$	f_{osc}	$\widetilde{\nu}_{v\leftarrow 0}$	f_{osc}	$\widetilde{\nu}_{v\leftarrow 0}$	f_{osc}	$\widetilde{\nu}_{v\leftarrow 0}$	f_{osc}
$\|3\rangle\|0\rangle\|0\rangle$	8564	6.99×10^{-10}	8502	7.35×10^{-10}	8455	7.06×10^{-10}		
$\|2\rangle\|1\rangle\|0\rangle$	8794	5.74×10^{-11}	8806	4.63×10^{-12}	8650	2.08×10^{-10}		
$\|1\rangle\|2\rangle\|0\rangle$	8901	1.20×10^{-10}	8705	8.25×10^{-11}	8768	6.61×10^{-11}		
$\|0\rangle\|3\rangle\|0\rangle$	8579	5.07×10^{-10}	8475	9.03×10^{-10}	8467	8.59×10^{-10}		
$\|2\rangle\|0\rangle\|1\rangle$	8798	1.73×10^{-10}	8784	6.86×10^{-11}	8704	1.12×10^{-10}		
$\|0\rangle\|2\rangle\|1\rangle$	8927	7.00×10^{-13}	8776	9.84×10^{-11}	8715	3.10×10^{-10}		
$\|1\rangle\|0\rangle\|2\rangle$	8894	1.39×10^{-11}	8698	2.79×10^{-10}	8799	4.72×10^{-11}		
$\|0\rangle\|1\rangle\|2\rangle$	8736	2.68×10^{-10}	8652	2.08×10^{-10}	8823	1.78×10^{-11}		
$\|0\rangle\|0\rangle\|3\rangle$	8585	5.31×10^{-10}	8468	6.81×10^{-10}	8544	8.79×10^{-10}		
$\Delta v = 3$ total		2.38×10^{-9}		3.07×10^{-9}		3.22×10^{-9}	8497	1.10×10^{-9}
$\|4\rangle\|0\rangle\|0\rangle$	11203	6.20×10^{-11}	11107	8.36×10^{-11}	11042	6.77×10^{-11}		
$\|3\rangle\|1\rangle\|0\rangle$	11474	4.78×10^{-12}	11477	7.54×10^{-13}	11360	3.37×10^{-12}		
$\|1\rangle\|3\rangle\|0\rangle$	11587	7.79×10^{-12}	11402	1.23×10^{-11}	11400	2.04×10^{-11}		
$\|0\rangle\|4\rangle\|0\rangle$	11221	6.02×10^{-11}	11069	8.70×10^{-11}	11058	8.62×10^{-11}		
$\|3\rangle\|0\rangle\|1\rangle$	11523	3.43×10^{-12}	11449	2.58×10^{-12}	11419	2.17×10^{-12}		
$\|0\rangle\|3\rangle\|1\rangle$	11526	1.23×10^{-11}	11367	4.60×10^{-12}	11442	4.24×10^{-12}		
$\|1\rangle\|0\rangle\|3\rangle$	11584	4.81×10^{-13}	11406	1.28×10^{-11}	11469	4.48×10^{-12}		
$\|0\rangle\|1\rangle\|3\rangle$	11618	1.12×10^{-13}	11445	5.48×10^{-12}	11507	2.23×10^{-12}		
$\|0\rangle\|0\rangle\|4\rangle$	11219	4.35×10^{-13}	11061	6.75×10^{-11}	11165	9.45×10^{-11}		
$\Delta v = 4$ total		1.97×10^{-10}		2.79×10^{-10}		2.87×10^{-10}	11086	8.94×10^{-11}
$\|5\rangle\|0\rangle\|0\rangle$	13720	6.27×10^{-12}	13591	9.34×10^{-12}	13508	7.05×10^{-12}		
$\|4\rangle\|1\rangle\|0\rangle$	14137	2.55×10^{-13}	14071	8.10×10^{-14}	13965	3.92×10^{-13}		
$\|1\rangle\|4\rangle\|0\rangle$	14164	6.98×10^{-13}	14039	1.63×10^{-14}	13981	1.29×10^{-12}		
$\|0\rangle\|5\rangle\|0\rangle$	13741	5.69×10^{-12}	13545	9.20×10^{-12}	13531	8.89×10^{-12}		
$\|4\rangle\|0\rangle\|1\rangle$	14206	1.76×10^{-13}	14020	1.13×10^{-12}	14020	1.01×10^{-13}		
$\|0\rangle\|4\rangle\|1\rangle$	14216	1.31×10^{-13}	13991	1.14×10^{-12}	14036	2.75×10^{-13}		
$\|1\rangle\|0\rangle\|4\rangle$	14231	2.80×10^{-14}	14031	2.49×10^{-13}	14076	3.49×10^{-13}		
$\|0\rangle\|1\rangle\|4\rangle$	14159	7.27×10^{-13}	13981	2.70×10^{-13}	14123	2.85×10^{-13}		
$\|0\rangle\|0\rangle\|5\rangle$	13741	4.57×10^{-12}	13533	6.94×10^{-12}	13667	9.19×10^{-12}		
$\Delta v = 5$ total		1.87×10^{-11}		2.85×10^{-11}		2.80×10^{-11}	13554	8.82×10^{-12}
$\|6\rangle\|0\rangle\|0\rangle$	16120	8.62×10^{-13}	15956	1.36×10^{-12}	15856	1.03×10^{-12}		
$\|5\rangle\|1\rangle\|0\rangle$	16728	7.65×10^{-15}	16557	8.08×10^{-15}	16436	7.51×10^{-14}		
$\|1\rangle\|5\rangle\|0\rangle$	16687	9.59×10^{-14}	16517	5.34×10^{-15}	16455	9.49×10^{-14}		
$\|0\rangle\|6\rangle\|0\rangle$	16144	8.98×10^{-13}	15901	1.24×10^{-12}	15884	1.22×10^{-12}		
$\|5\rangle\|0\rangle\|1\rangle$	16667	6.38×10^{-14}	16509	9.76×10^{-14}	16489	1.44×10^{-14}		
$\|0\rangle\|5\rangle\|1\rangle$	16745	7.44×10^{-15}	16468	1.24×10^{-13}	16510	2.19×10^{-14}		
$\|1\rangle\|0\rangle\|5\rangle$	16684	2.85×10^{-14}	16505	2.38×10^{-14}	16581	3.21×10^{-14}		
$\|0\rangle\|1\rangle\|5\rangle$	16749	1.04×10^{-14}	16458	2.81×10^{-14}	16629	2.82×10^{-14}		
$\|0\rangle\|0\rangle\|6\rangle$	16144	7.29×10^{-13}	15886	9.51×10^{-13}	16050	1.28×10^{-12}		
$\Delta v = 6$ total		2.72×10^{-12}		3.85×10^{-12}		3.80×10^{-12}	15901	1.10×10^{-12}

[a] An 11 point grid was used to calculate the dipole moment function derivatives in Equation (14).

Table 4. Transition frequencies (in cm^{-1}), $\tilde{\nu}_{v\leftarrow 0}$, and oscillator strengths, f_{osc}, of the HCAO calculated[a] CH vibrational overtone transitions $\Delta v = 3 - 6$ in conformer II of sarin

	$\|CH_1\rangle\|CH_2\rangle\|CH_3\rangle$		$\|CH_4\rangle\|CH_5\rangle\|CH_6\rangle$		$\|CH_7\rangle\|CH_8\rangle\|CH_9\rangle$		$\|CH_{10}\rangle$	
State	$\tilde{\nu}_{v\leftarrow 0}$	f_{osc}	$\tilde{\nu}_{v\leftarrow 0}$	f_{osc}	$\tilde{\nu}_{v\leftarrow 0}$	f_{osc}	$\tilde{\nu}_{v\leftarrow 0}$	f_{osc}
$\|3\rangle\|0\rangle\|0\rangle$	8556	6.62×10^{-10}	8510	8.55×10^{-10}	8465	6.63×10^{-10}		
$\|2\rangle\|1\rangle\|0\rangle$	8789	5.34×10^{-11}	8809	8.83×10^{-12}	8649	2.07×10^{-10}		
$\|1\rangle\|2\rangle\|0\rangle$	8897	1.14×10^{-10}	8699	2.93×10^{-10}	8775	6.02×10^{-11}		
$\|0\rangle\|3\rangle\|0\rangle$	8581	5.42×10^{-10}	8472	8.99×10^{-10}	8478	8.03×10^{-10}		
$\|2\rangle\|0\rangle\|1\rangle$	8994	1.28×10^{-11}	8787	8.58×10^{-10}	8697	1.33×10^{-10}		
$\|0\rangle\|2\rangle\|1\rangle$	8923	2.24×10^{-12}	8774	8.06×10^{-11}	8703	2.79×10^{-10}		
$\|1\rangle\|0\rangle\|2\rangle$	8888	1.77×10^{-11}	8707	9.66×10^{-11}	8786	3.88×10^{-11}		
$\|0\rangle\|1\rangle\|2\rangle$	8793	1.73×10^{-10}	8652	2.28×10^{-10}	8808	5.78×10^{-11}		
$\|0\rangle\|0\rangle\|3\rangle$	8574	4.97×10^{-10}	8467	7.02×10^{-10}	8498	7.29×10^{-10}		
$\Delta v = 3$ total		2.33×10^{-9}		3.26×10^{-9}		2.99×10^{-9}	8561	1.27×10^{-9}
$\|4\rangle\|0\rangle\|0\rangle$	11189	7.69×10^{-11}	11119	8.15×10^{-11}	11057	7.16×10^{-11}		
$\|3\rangle\|1\rangle\|0\rangle$	11466	5.78×10^{-12}	11482	9.80×10^{-13}	11364	3.99×10^{-12}		
$\|1\rangle\|3\rangle\|0\rangle$	11580	7.64×10^{-12}	11402	1.01×10^{-11}	11399	2.31×10^{-11}		
$\|0\rangle\|4\rangle\|0\rangle$	11216	5.24×10^{-11}	11065	8.59×10^{-11}	11074	9.98×10^{-11}		
$\|3\rangle\|0\rangle\|1\rangle$	11515	4.41×10^{-12}	11452	5.37×10^{-12}	11443	1.33×10^{-12}		
$\|0\rangle\|3\rangle\|1\rangle$	11518	1.10×10^{-11}	11367	5.36×10^{-12}	11449	3.03×10^{-12}		
$\|1\rangle\|0\rangle\|3\rangle$	11576	2.92×10^{-13}	11410	1.50×10^{-11}	11404	5.17×10^{-12}		
$\|0\rangle\|1\rangle\|3\rangle$	11611	2.38×10^{-13}	11445	2.64×10^{-12}	11475	4.44×10^{-12}		
$\|0\rangle\|0\rangle\|4\rangle$	11213	5.02×10^{-11}	11060	7.14×10^{-11}	11100	8.09×10^{-11}		
$\Delta v = 4$ total		2.11×10^{-10}		2.80×10^{-10}		2.96×10^{-10}	11175	9.98×10^{-11}
$\|5\rangle\|0\rangle\|0\rangle$	13701	6.43×10^{-12}	13607	9.17×10^{-12}	13528	6.86×10^{-12}		
$\|4\rangle\|1\rangle\|0\rangle$	14124	3.58×10^{-13}	14027	8.06×10^{-13}	13977	4.75×10^{-13}		
$\|1\rangle\|4\rangle\|0\rangle$	14157	6.75×10^{-13}	14038	3.63×10^{-13}	13993	1.40×10^{-12}		
$\|0\rangle\|5\rangle\|0\rangle$	13736	5.34×10^{-12}	13539	9.09×10^{-12}	13551	8.96×10^{-12}		
$\|4\rangle\|0\rangle\|1\rangle$	14193	2.12×10^{-13}	14081	8.90×10^{-14}	14028	1.77×10^{-13}		
$\|0\rangle\|4\rangle\|1\rangle$	14207	1.27×10^{-13}	13989	1.11×10^{-12}	14044	8.79×10^{-14}		
$\|1\rangle\|0\rangle\|4\rangle$	14149	5.89×10^{-13}	14035	2.05×10^{-13}	14014	2.92×10^{-13}		
$\|0\rangle\|1\rangle\|4\rangle$	14223	3.48×10^{-14}	13979	3.51×10^{-13}	14064	4.80×10^{-13}		
$\|0\rangle\|0\rangle\|5\rangle$	13731	4.79×10^{-12}	13532	7.07×10^{-12}	13583	9.03×10^{-12}		
$\Delta v = 5$ total		1.87×10^{-11}		2.84×10^{-11}		2.79×10^{-11}	13669	9.46×10^{-12}
$\|6\rangle\|0\rangle\|0\rangle$	16095	1.13×10^{-12}	15977	1.19×10^{-12}	15880	1.01×10^{-12}		
$\|5\rangle\|1\rangle\|0\rangle$	16709	8.17×10^{-15}	16573	8.88×10^{-15}	16452	8.29×10^{-14}		
$\|1\rangle\|5\rangle\|0\rangle$	16679	8.58×10^{-14}	16512	6.38×10^{-15}	16472	1.06×10^{-13}		
$\|0\rangle\|6\rangle\|0\rangle$	16138	7.84×10^{-13}	15894	1.27×10^{-12}	15909	1.30×10^{-12}		
$\|5\rangle\|0\rangle\|1\rangle$	16647	8.07×10^{-14}	16525	9.57×10^{-14}	16501	1.26×10^{-15}		
$\|0\rangle\|5\rangle\|1\rangle$	16739	1.82×10^{-15}	16463	1.30×10^{-13}	16524	8.22×10^{-15}		
$\|1\rangle\|0\rangle\|5\rangle$	16673	2.18×10^{-14}	16506	1.95×10^{-14}	16502	4.62×10^{-14}		
$\|0\rangle\|1\rangle\|5\rangle$	16736	1.75×10^{-14}	16457	3.00×10^{-14}	16549	4.96×10^{-14}		
$\|0\rangle\|0\rangle\|6\rangle$	16132	7.50×10^{-13}	15885	9.98×10^{-13}	15946	1.34×10^{-12}		
$\Delta v = 6$ total		2.89×10^{-12}		3.76×10^{-12}		3.95×10^{-12}	16043	1.14×10^{-12}

[a] An 11 point grid was used to calculate the dipole moment function derivatives in Equation (14).

ACKNOWLEDGMENTS

Many thanks are owed to Prof. Henrik Kjaergaard and to Dr. Daryl Howard for their assistance with the interpretation of vibrational overtone state identities.

This research has been enabled by the use of WestGrid computing resources, which are funded in part by the Canada Foundation for Innovation, Alberta Innovation and Science, B. C. Advanced Education, and the participating research institutions. Specifically, the *ab initio* calculations presented in this paper were run on `lattice.westgrid.ca`, which is located at and supported by the University of Calgary.

REFERENCES

1. O. S. Mortensen, B. R. Henry, and M. A. Mohammadi, "The effects of symmetry within the local mode picture: A reanalysis of the overtone spectra of the dihalomethanes," *J. Chem. Phys.* **75**, pp. 4800–4808, Nov. 15 1981.
2. M. S. Child and T. R. Lawton, "Local and normal vibrational states: a harmonically coupled anharmonic-oscillator model," *Faraday Discuss. Chem. Soc.* **71**, pp. 273–285, 1981.
3. H. G. Kjaergaard, C. D. Daub, and B. R. Henry, "The role of electron correlation on calculated XH-stretching vibrational band intensities," *Mol. Phys.* **90**(2), pp. 201–213, 1997.
4. H. G. Kjaergaard, K. J. Bezar, and K. A. Brooking, "Calculation of dipole moment functions with density functional theory: application to vibrational band intensities," *Mol. Phys.* **96**(7), pp. 1125–1138, 1999.
5. D. J. Donaldson, J. J. Orlando, S. Amann, G. S. Tyndall, R. J. Proos, B. R. Henry, and V. Vaida, "Absolute intensities of nitric acid overtones," *J. Phys. Chem. A* **102**, pp. 5171–5174, July 2 1998.
6. M. G. Sowa, B. R. Henry, and Y. Mizugai, "Vibrational overtone study of 5-membered aromatic heterocycles: Fermi resonance interactions," *J. Phys. Chem.* **97**, pp. 809–815, 1993.
7. G. R. Low and H. G. Kjaergaard, "Calculation of OH-stretching band intensities of the water dimer and trimer," *J. Chem. Phys.* **110**, pp. 9104–9115, May 8 1999.
8. B. R. Henry and H. G. Kjaergaard, "Local modes," *Can. J. Chem.* **80**, pp. 1635–1642, Dec. 2002.
9. R. J. Hayward and B. R. Henry, "A general local-mode theory for high energy polyatomic overtone spectra and application to dichloromethane," *J. Mol. Spectrosc.* **57**, pp. 221–235, 1975.
10. B. R. Henry, "The use of local modes in the description of highly vibrationally excited molecules," *Accounts Chem. Res.* **10**, pp. 207–213, 1977.
11. M. L. Sage and J. Jortner, "Bond modes," *Adv. Chem. Phys.* **47**, pp. 293–322, 1981.
12. B. R. Henry, "The local mode model," in *Vibrational Spectra and Structure*, J. R. Durig, ed., **10**, pp. 269–319, Elsevier Scientific, Amsterdam, 1981.
13. B. R. Henry, A. W. Tarr, O. S. Mortensen, W. F. Murphy, and D. A. C. Compton, "Raman and infrared excitation of local modes in neopentane," *J. Chem. Phys.* **79**, pp. 2583–2589, Sept. 15 1983.
14. M. S. Child and L. Halonen, "Overtone frequencies and intensities in the local mode picture," *Adv. Chem. Phys.* **57**, pp. 1–58, 1984.
15. E. B. Wilson, Jr, J. C. Decius, and P. C. Cross, *Molecular Vibrations; the Theory of Infrared and Raman Vibrational Spectra*, McGraw-Hill, New York, 1955.
16. H. G. Kjaergaard, B. R. Henry, H. Wei, S. Lefebvre, T. Carrington, Jr, and O. S. Mortensen, "Calculation of vibrational fundamental and overtone band intensities of H_2O," *J. Chem. Phys.* **100**, pp. 6228–6239, May 1 1994.
17. M. G. Sowa, B. R. Henry, and Y. Mizugai, "Vibrational overtone study of 5-membered aromatic heterocycles: Local mode interpretations," *J. Phys. Chem.* **95**(20), pp. 7659–7664, 1991.
18. M. W. P. Petryk and B. R. Henry, "CH stretching vibrational overtone spectra of *tert*-butylbenzene, *tert*-butyl chloride, and *tert*-butyl iodide," *J. Phys. Chem. A* **109**, pp. 4081–4091, May 12 2005.
19. P. W. Atkins, *Molecular Quantum Mechanics*, Oxford University Press, Oxford, 2^{nd} ed., 1983.
20. E. R. Cohen and B. N. Taylor, "Fundamental physical constants," *J. Res. Natl. Bur. Stand.* **92**, p. 85, 1987.
21. H. G. Kjaergaard, *Local Mode Spectroscopy: Calculation and Measurement of Overtone Intensities.* PhD thesis, Odense University, Denmark, 1992.

22. H. G. Kjaergaard, H. Yu, B. J. Schattka, B. R. Henry, and A. W. Tarr, "Intensities in local mode overtone spectra: Propane," *J. Chem. Phys.* **93**, pp. 6239–6248, Nov. 1 1990.
23. O. S. Mortensen, M. K. Ahmed, B. R. Henry, and A. W. Tarr, "Intensities in local mode overtone spectra: Dichloromethane and deuterated dichloromethane," *J. Chem. Phys.* **82**, pp. 3903–3911, 1985.
24. A. W. Tarr, D. J. Swanton, and B. R. Henry, "Scf calculations of the ch-stretching overtone intensities in dichloromethane within the local mode model," *J. Chem. Phys.* **85**, pp. 3463–3468, 1986.
25. H. G. Kjaergaard, B. R. Henry, and A. W. Tarr, "Intensities in local mode overtone spectra of dimethyl ether and acetone," *J. Chem. Phys.* **94**, pp. 5844–5854, 1991.
26. H. G. Kjaergaard and B. R. Henry, "*Ab initio* calcuation of dipole moment functions: application to vibrational band intensities of H_2O," *Mol. Phys.* **83**, pp. 1099–1116, Dec. 20 1994.
27. C. D. Daub, B. R. Henry, M. L. Sage, and H. G. Kjaergaard, "Modeling and calculation of dipole moment functions for XH bonds," *Can. J. Chem.* **77**, pp. 1775–1781, Nov. 1999.
28. M. J. Frisch *et al.*, "Gaussian 03, Revision C.02," 2004.
29. A. Kaczmarek, L. Gorb, A. J. Sadlej, and J. Leszczynski, "Sarin and soman: Structure and properties," *Struct. Chem.* **15**, pp. 517–525, Oct. 2004.
30. L. Pauling, *The Nature of the Chemical Bond*, Cornell University Press, Ithaca, N. Y., 3^{rd} ed., 1960.
31. B. R. Henry and R. J. D. Miller, "Intramolecular perturbations of CH-stretching diagonal local mode anharmonicity in methyl substituted alkanes," *Chem. Phys. Lett.* **60**, pp. 81–84, Dec. 15 1978.
32. M. A. Mohammadi and B. R. Henry, "Nonbonded interaction potentials in methyl-substituted butanes, obtained from high-energy overtone spectra," *Proc. Natl. Acad. Sci. USA* **78**, pp. 686–688, Feb. 1981.
33. B. R. Henry, M. A. Mohammadi, and J. A. Thomson, "Intramolecular and intermolecular interactions in methyl substituted pentanes as revealed by high energy CH-stretching overtone spectra," *J. Chem. Phys.* **75**, pp. 3165–3174, Oct. 1 1981.
34. M. W. P. Petryk and B. R. Henry, "Through space coupling and fermi resonances in neopentane-d_0, -d_6, -d_9, and tetramethylsilane," *J. Phys. Chem. A* **106**, pp. 8599–8608, Sept. 19 2002.
35. M. W. P. Petryk, B. R. Henry, and M. L. Sage, "Site–site potentials in neopentane and tetramethylsilane," *J. Phys. Chem. A* **109**, pp. 9969–9979, Nov. 10 2005.
36. D. J. Nesbitt and R. W. Field, "Vibrational energy flow in highly excited molecules: Role of intramolecular vibrational energy redistribution," *J. Phys. Chem.* **100**, pp. 12735–12756, Aug. 1 1996.
37. A. R. Hight Walker, R. D. Suenram, A. Samuels, J. Jensen, M. W. Ellzy, J. M. Lochner, and D. Zeroka, "Rotational spectrum of sarin[1]," *J. Mol. Spectrosc.* **207**, pp. 77–82, May 2001.
38. C. Zhu, H. G. Kjaergaard, and B. R. Henry, "CH-stretching overtone spectra and internal methyl rotation in 2,6-difluorotoluene," *J. Chem. Phys.* **107**, pp. 691–701, July 15 1997.
39. Z. Rong, C. Zhu, and B. R. Henry, "CH stretching overtone spectra of fluorine substituted toluenes," *J. Phys. Chem. A* **107**, pp. 10771–10780, Dec. 11 2003.
40. D. P. Schofield and H. G. Kjaergaard, "Effect of OH internal torsion on the OH-stretching spectrum of *cis,cis*-HOONO," *J. Phys. Chem. A* **109**, pp. 1810–1814, Mar. 10 2005.
41. W. Kaye, "Near-infrared spectroscopy: I. spectral identification and analytical applications," *Spectrochim. Acta* **6**, pp. 257–287, Sept. 1954.
42. B. R. Henry and I.-F. Hung, "Mass effects on the applicability of a local mode description—an analysis of the high energy overtone spectra of difluoro-, dichloro-, dibromo-, and diiodomethane," *Chem. Phys.* **29**, pp. 465–475, Apr. 1 1978.
43. M. W. P. Petryk and B. R. Henry, "CH stretching vibrational overtone spectra of 1,3,5,7-cyclooctatetraene and 1,1,1-trichloroethane," *J. Phys. Chem. A* **109**, pp. 7113–7120, Aug. 18 2005.